Phase relaxation of Faraday surface waves

A.V. Kityk,[1,4] C. Wagner,[2] K. Knorr,[1] and H. W. Müller[1,3]
[1]*Fakultät für Physik und Elektrotechnik, Universität des Saarlandes, 66041 Saarbrücken, Germany*
[2]*Laboratoire de Physique Statistique, Ecole Normale Supérieure, 24 rue Lhomond, 75231 Paris Cedex 05, France*
[3]*Max-Planck-Institut für Polymerforschung, Ackermannweg 10, 55128 Mainz, Germany*
[4]*Electrical Engineering Department, Czestochowa Technical University, Al. Armii Krajowej 17, PL-42200 Czestochowa, Poland*
(Received 13 September 2001; published 18 June 2002)

Surface waves on a liquid-air interface excited by a vertical vibration of a fluid layer (Faraday waves) are employed to investigate the phase relaxation of ideally ordered patterns. By means of a combined frequency-amplitude modulation of the excitation signal a periodic expansion and dilatation of a square wave pattern is generated, the dynamics of which is well described by a Debye relaxator. By comparison with the results of a linear theory, it is shown that the measured relaxation time allows a precise evaluation of the phase diffusion constant.

DOI: 10.1103/PhysRevE.65.066304 PACS number(s): 47.54.+r, 47.20.Ma

Our understanding of spatiotemporal pattern formation in nonequilibrium fluid systems has greatly benefited [1] from recent quantitative experiments in combination with the development of new theoretical concepts. One of them is the so-called *amplitude equation* approach [2], which is based on the linear instability of a homogeneous state and leads naturally to a classification of patterns in terms of characteristic wave numbers and frequencies. A different but equally universal description, the *phase dynamics* [3], applies to situations where a periodic spatial pattern experiences long-wavelength phase modulations. This approach, originally introduced in the context of thermal convection, has proven to be useful to understand the stability and the relaxation of periodic patterns, wave number selection, and defect dynamics. In many paradigmatic pattern forming systems such as thermal convection in a fluid layer heated from below (Rayleigh-Bénard convection, RBC) or the formation of azimuthal vortices in the gap between two rotating cylinders (Taylor-Couette flow, TCF) the dominating wave number is dictated by the geometry and thus inconvenient to be changed in a given experimental setup (for instance by a mechanical ramp of the layer thickness [4]).

Faraday waves are surface waves on the interface between two immiscible fluids, excited by a vertical vibration of the container. Beyond a sufficiently large excitation amplitude the plane interface undergoes an instability (Faraday instability) and standing surface waves appear, oscillating with a frequency one-half of the drive. This type of parametric wave instability is attractive as the wavelength of the pattern is *dispersion* rather than *geometry* controlled. Just by varying the drive frequency the wave number can be tuned in a wide range. In that sense the Faraday setup is well suited for the study of phase dynamics.

Nevertheless recent research activity in this field was mainly dedicated to the exploration of the processes underlying the selection of patterns with a fixed wavelength. Faraday [5] was the first to provide a quantitative study of this system, revealing that a sinusoidal vibration may induce a periodic array of squares. Later on, more complicated patterns with up to a 12-fold rotational symmetry (quasiperiodic structures) have been observed [6,7]. Here the amplitude equation technique contributed considerably to unfold the governing spatiotemporal resonance mechanisms. Applied to a set of modes $\mathbf{k}_i$ with different orientations but fixed wavelength, $|\mathbf{k}_i|=k$, the resulting set of Landau equations lead to a semiquantitative understanding [8] of pattern selection in this system. Motivated by these advances the idea came up to apply more complicated drive signals composed of two or more commensurable frequencies [9]. That way the simultaneous excitation of distinct wavelengths gave rise to novel surface patterns in the form of superlattices [9–11]. Only recently, the phase information carried by the participating modes was found to have a crucial influence on the visual appearance of the convection structures [12].

In comparison to other classical pattern forming systems such as RBC or TCF, the phase dynamics in the Faraday system is much less explored. In usual Faraday experiments the drive frequency (or frequency composition including relative amplitudes) is held fixed while the overall drive amplitude is ramped in order to record the bifurcation sequence of appearing structures. To our knowledge none of the previous investigations used the excitation frequency ω as the primary control parameter rather than the drive amplitude a. That way it is particularly simple to impose phase perturbations on ordered patterns and to study their relaxation dynamics. Moreover, doing phase dynamics on the Faraday system has the additional advantage of rather quick relaxation times, which in typical setups are one and two orders of magnitude faster than for instance in RBC.

The present paper reports a systematic investigation of phase relaxation on Faraday surface waves. Our study is focused on the relaxational dynamics of an ideal surface pattern with a square tesselation. By evaluating the relaxation time of the pattern in response to small changes of the frequency, the phase diffusion coefficient has been measured. The experimental results are found to be in good agreement with the predictions of the linear theory [3,4], which we evaluated for a system of infinite lateral extension.

The experimental setup consists of a black cylindrical container built out of anodized aluminum, and filled to a height h of 4.2 mm with a silicone oil (kinematic viscosity $\nu=21.4\times10^{-6}$ m^2/s, density $\rho=949$ kg/m^3, surface ten-

 ©2002 The American Physical Society

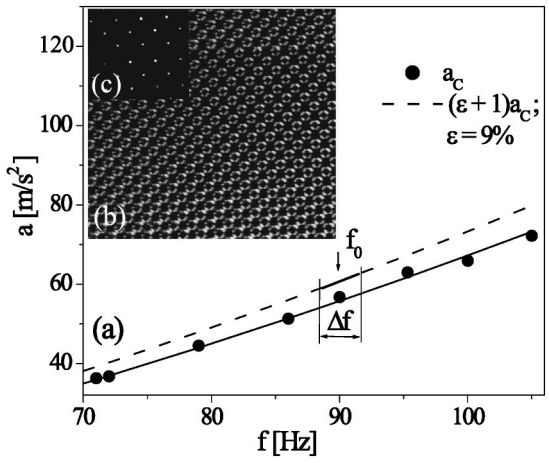

FIG. 1. (a) Symbols denote the critical acceleration amplitude a_c as measured at the onset of the Faraday instability at constant drive frequency $\omega=2\pi f$. The solid line indicates the theoretical prediction for the material parameters given. Along the dashed line the reduced drive amplitude is $\varepsilon=9\%$. The phase relaxation experiments were performed by imposing simultaneous small changes of f and a, as indicated for an example by the solid bar. (b) and (c) show a square pattern and the associated two-dimensional power spectrum as observed during the modulation experiments.

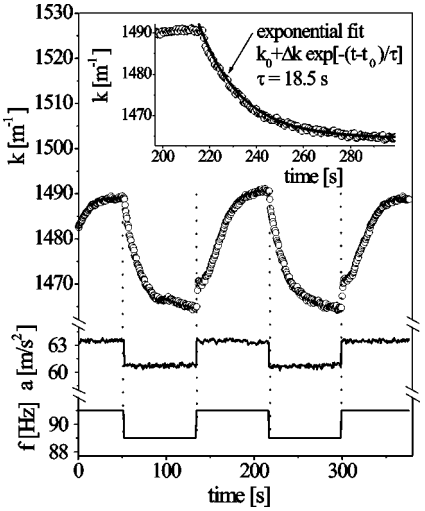

FIG. 2. Temporal decay of the wave number $k(t)$ in response to a steplike [type (i)] change of the drive frequency f. Also the drive amplitude a was changed to keep the reduced amplitude $\varepsilon=a(t)/a_c[\omega(t)]-1$ constant. The decay of the wave number $k(t)$ could be fitted by an exponential. (Parameters: $L=0.265$ m, $\varepsilon=9\%$, $f=90$ Hz.)

sion $\sigma=17.3\times10^{-3}$ N/m). The lateral boundaries of our container have a beachlike shape; the angle of which was adapted such as to avoid the formation of a meniscus. Phase pinning effects were thus avoided, actually we found no experimental evidences for it. In order to study finite size effects, we used three different containers, with inner diameters $L_1=265$ mm, $L_2=185$ mm, and $L_3=125$ mm. A glass plate covering the container was used to prevent evaporation, pollution, and temperature fluctuations of the liquid. Furthermore, to avoid uncontrolled changes of the viscosity, density, and surface tension of the liquid, all the measurements have been performed at a constant temperature of 30 ±0.1°C. The Faraday waves were excited by an electromagnetic shaker vibrating vertically with an acceleration allowing for simultaneous amplitude *and* frequency modulations in the form $a(t)\cos\omega(t)$. The corresponding input signal was produced by a wave form generator via a digital to analog converter. The instantaneous acceleration was measured by a piezoelectric sensor. In a preparatory experiment undertaken with a sinusoidal (i.e., unmodulated) drive $a\cos\omega t$ the critical acceleration amplitude $a_c(\omega)$ for the onset of the Faraday instability was determined by visual inspection of the interface while quasistatically ramping a at fixed $\omega=2\pi f$ (see Fig. 1). Throughout the investigated frequency interval 70 Hz$<f<$110 Hz the surface patterns, which appear at a supercritical drive of less than about $1.1\times a_c$, always consisted of an ordered square wave pattern, which—after some healing time—was free of defects [Fig. 1(b)]. In order to study the dynamics of phase-perturbed patterns we have carried out measurements of the average wave number $k(t)$ of the Faraday pattern in response to small changes of the drive frequency $\omega(t)$ around a mean value ω_0. The ω modulation has been accomplished in two different ways. (i) By discontinuous jumps (back and forth) between frequencies $\omega_0-\Delta\omega/2$ and $\omega_0+\Delta\omega/2$ with a repetition period T between 100 and 300 s, sufficiently large for the pattern to relax. (ii) By a sinusoidal modulation of the drive frequency according to $\omega(t)=\omega_0+\Delta\omega\sin(\Omega t)$, with $T=1/F=2\pi/\Omega$ between 2 and 1000 s (within the frequency range of our study, the response time of the shaker to small changes of the drive frequency is less than 10 ms and thus negligible). In both cases the vibration amplitude $a(t)$ was comodulated in such a way that the instantaneous supercritical drive $\varepsilon=a(t)/a_c[\omega(t)]-1$ remained constant [see Fig. 1(a)]. The bandwidth $\Delta\omega$ of the modulation needed to be confined to a few Hz in order to avoid the occurrence of dislocation-type defects. Under such conditions the square pattern remained practically ideal without perturbations [see Fig. 1(b)], just expanding and contracting (breathing) in a homogeneous manner with the modulation period T. To obtain the temporal wave number dependence a full frame CCD camera surrounded by a set of four incandescent lamps was mounted some distance above the container. About 100 pictures of the light reflected from the surface were taken at consecutive instances of maximum surface excursion from which the spatially averaged wave number $k(t)$ was extracted by evaluating the position of the principal peaks in a two-dimensional fast Fourier transform.

The wave number $k(t)$ followed the modulation in a relaxational manner. For the discontinuous modulation (i) this is directly apparent from Fig. 2. Here the relaxation time τ has been derived by fitting the exponential decay of the data. In the type (ii) experiment $k(t)$ oscillates around a mean value k_0 with an amplitude Δk_m and a temporal phase lag δ (see Fig. 3). Introducing the complex wave number increment $\Delta k^\star=\mathrm{Re}[\Delta k^\star]+i\,\mathrm{Im}[\Delta k^\star]=\Delta k_m e^{i\delta}$, its real and imaginary parts are plotted in Fig. 4 as a function of the modulation frequency F. The solid curves of this figure are fits of a linear Debye relaxator [13], where $\Delta k^*=\Delta k(\Omega$

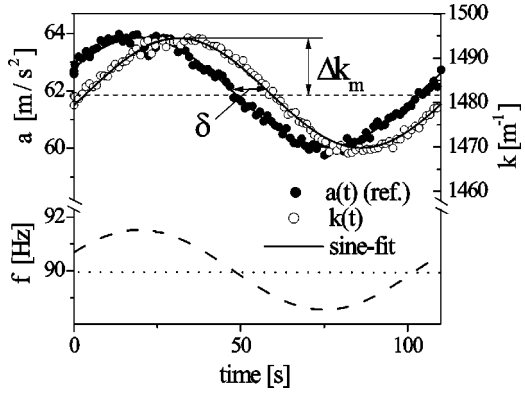

FIG. 3. Relaxational dynamics of the wave number $k(t)$ in response to a sinusoidal [type (ii)] modulation of the drive frequency. The drive amplitude a was comodulated to keep the reduced amplitude ε constant. The Faraday pattern responds with a sinusoidal variation of its instantaneous wave number $k(t)$ with an amplitude Δk_m and a temporal phase lag δ (parameters: $L=0.265$ m, $\varepsilon=9\%$, and $f=90$ Hz).

$=0)/[1+i\Omega\tau]$. Figure 5 shows the relaxation time τ, as obtained from both types of experiments, as a function of the mean wave number k_0, the container diameter L, and the reduced drive strength ε. A dependence on the (small) modulation amplitude $\Delta\omega$ could not be detected. The experimental data reveal a linear increase with the wave number k_0 and a proportionality to the square of the container size L.

The dependence of the relaxation time τ on, respectively, k_0, L, and ε can be understood in terms of the phase diffusion approach [3]. Here one takes advantage of the fact that local disturbances of the elevation amplitude die out rapidly, while long-wavelength phase perturbation survive on a much longer (diffusive) time scale. To streamline the arguments and to work out the basic physics we consider a one-dimensional surface elevation profile in the form of stripes as given by $\zeta(x,t)\propto[e^{ik_0x+\varphi(x,t)}+\text{c.c.}]\cos(\omega t/2)$. Here $\partial_x\varphi=\Delta k$ describes the spatiotemporal variation of the local wave number around the underlying base pattern with the

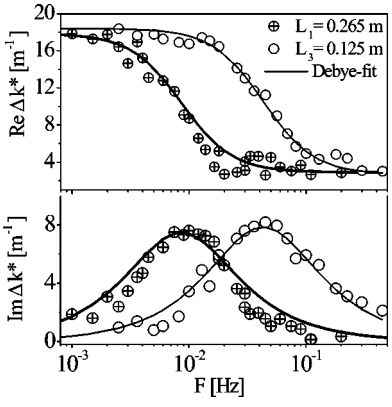

FIG. 4. Frequency "dispersion" of the real and imaginary parts of Δk^* as obtained from modulation experiments of type (ii) for the two different container diameters $L_1=265$ mm and $L_3=125$ mm ($f=90$ Hz, $k_0=1480$ m^{-1}, and $\varepsilon=9\%$). Solid curves are fits according to the Debye relaxator.

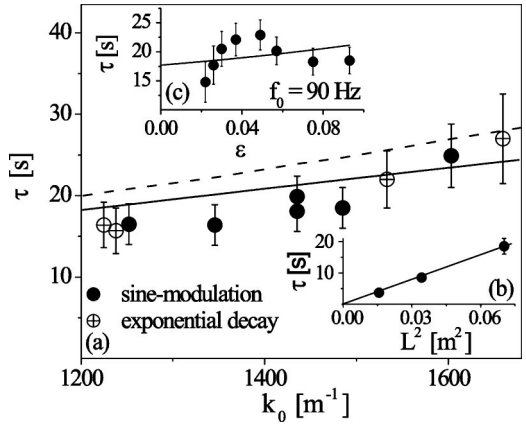

FIG. 5. The characteristic relaxation time τ as a function of (a) the mean wave number k_0, (b) the container size L, and (c) the reduced drive strength ε. The dashed line shows the prediction for infinite depth capillary waves [Eq. (2)], while the solid line is based on a numerical evaluation for the (more realistic) case of finite depth gravity-capillary waves. (Parameters: $L=0.265$ m, $\varepsilon=9\%$, and $f=90$ Hz.)

wave number k_0. Following the phase diffusion approach the phase φ obeys a diffusion equation of the form $\partial_t\varphi=D_\parallel\partial_{xx}\varphi$ with the diffusion constant (valid just above onset) of the form

$$D_\parallel=\frac{\xi_0^2}{\tau_0}\,\frac{\varepsilon-3\xi_0^2(k_0-k_c)^2}{\varepsilon-\xi_0^2(k_0-k_c)^2}. \tag{1}$$

The coefficients $\tau_0^{-1}=\partial\lambda/\partial\varepsilon|_{k=k_c,\varepsilon=0}$ and $\xi_0^2=-\tau_0/2(\partial^2\lambda/\partial k^2)|_{k=k_c,\varepsilon=0}$ are given in terms of the linear growth rate $\lambda=\lambda(\varepsilon,k)$ at which planar wave perturbations grow out of the plane undeformed interface, when the Faraday instability sets in. Here k_c is the wave number at onset of the Faraday instability. For weakly damped ($\nu k_0^2/\omega\ll1$) capillary waves [$k_0\simeq(\rho/\sigma)^{1/3}(\omega/2)^{2/3}$] on a deep ($kh\gg1$) fluid layer (reasonable approximations in our experiment) one obtains approximately $\tau_0^{-1}\simeq2\nu k_0^2$ and $\xi_0^2=(1/2)[9\sigma/(16\nu^2\rho)]k_0^{-3}$. By decomposition of the phase perturbations into a set of discrete Fourier modes compatible with the finite container dimension, $\varphi=\Sigma_{n=1}^{\infty}a_n\sin(n\pi/L)$, the mode $n=1$ has the slowest decay time

$$\tau=\frac{L^2}{\pi^2}D_\parallel^{-1}=\frac{\nu\rho}{\sigma}k_0\frac{16L^2}{9\pi^2}\,\frac{\varepsilon-\xi_0^2(k_0-k_c)^2}{\varepsilon-3\xi_0^2(k_0-k_c)^2}, \tag{2}$$

and thus determines the relaxation time of the wave number of the experiment. The dashed line in Fig. 5 is the prediction according to Eq. (2). For a quantitatively more reliable check we also evaluated the coefficients τ_0 and ξ_0^2 numerically from a linear analysis, which takes into account the finite filling level as well as gravitational contributions to the wave dispersion. The respective result is shown by the solid line in Fig. 5(a). Furthermore, the predicted quadratic dependence of τ on the container dimension L is verified by Fig. 5(b). The theoretical prediction Eq. (2) also implies a slight depen-

dence of τ on the drive amplitude ε. However, checking for this feature requires to account for the fact that the mean wave number k_0 is also affected by the drive strength. We deduced the empiric dependence $k_0/k_c = 1-\beta\varepsilon$ with $\beta = 0.264$ from a control run where ε was slowly ramped at fixed f. Inserting this result into the last term on the right-hand side of Eq. (2) leads to the following expression:

$$\frac{\tau(\varepsilon)}{\tau(\varepsilon=0)} = \frac{1-\xi_0^2 k_c^2 \beta^2 \varepsilon}{1-3\xi_0^2 k_c^2 \beta^2 \varepsilon}. \tag{3}$$

Although this relation [see solid line in Fig. 5(c)] gives a reasonable estimate for the ε-dependence of τ it does not correctly reflect the empiric dependence. Apparently this is a finite size effect, which is expected to become significant at small values of ε. Roth *et al*. [14] recently demonstrated that the effective phase diffusion constant, measurable in RBC and TCF relaxation experiments, depends sensitively on the aspect ratio $\alpha = \sqrt{\varepsilon} L/\xi_0$, defined by the quotient between the container dimension and the linear correlation length. Taking TCF as an example, a decrease of α from 50 down to 15 (which in our experiment corresponds to a reduction of ε form 9% to 2%) implies a decay of the relaxation time by 20–30%. This is of the same order of magnitude as the value observed in our measurements [see Fig. 5(c)].

ACKNOWLEDGMENTS

We thank M. Lücke for helpful comments and J. Albers for his support. This work is supported by the Deutsche Forschungsgemeinschaft.

[1] M.C. Cross and P.C. Hohenberg, Rev. Mod. Phys. **65**, 851 (1993).

[2] A.C. Newell and J.A. Whitehead, J. Fluid Mech. **38**, 279 (1969); L.A. Segel, *ibid.* **38**, 203 (1969).

[3] Y. Pomeau and P. Manneville, J. Phys. (France) Lett. **40**, L-609 (1979).

[4] L. Kramer, E. Ben-Jacob, H. Brand, and M.C. Cross, Phys. Rev. Lett. **49**, 1891 (1982); Y. Pomeau and S. Zaleski, J. Phys. (France) Lett. **44**, L135 (1983); I. Rehberg, E. Bodenschatz, B. Winkler, and F.H. Busse, Phys. Rev. Lett. **59**, 282 (1987); L. Ning, G. Ahlers, and D.S. Cannell, *ibid.* **64**, 1235 (1990).

[5] M. Faraday, Philos. Trans. R. Soc. London **52**, 319 (1831).

[6] S. Douady, J. Fluid Mech. **221**, 383 (1990); B. Christiansen, P. Alstrom, and M.T. Levinsen, Phys. Rev. Lett. **68**, 2157 (1992); J. Fluid Mech. **291**, 3231 (1998); K. Kumar and K.M.S. Bajaj, Phys. Rev. E **52**, R4606 (1995); A. Kudrolli and J.P. Gollub, Physica D **97**, 133 (1996); D. Binks and W. van der Water, Phys. Rev. Lett. **78**, 4043 (1997).

[7] For a recent review see also: H.W. Müller, R. Friedrich, and D. Papathanassiou, in *Theoretical and Experimental Studies of the Faraday Instability*, edited by F. Busse and S.C. Müller, Lecture Notes in Physics, Vol. 55 (Springer, Berlin, 1998).

[8] S.T. Milner, J. Fluid Mech. **225**, 81 (1991); W. Zhang and J. Vinals, Phys. Rev. E **53**, R4283 (1996); J. Fluid Mech. **336**, 301 (1997); **341**, 225 (1997); P. Chen and J. Vinals, Phys. Rev. Lett. **79**, 2670 (1997); Phys. Rev. E **60**, 559 (1999).

[9] W.S. Edwards and S. Fauve, Phys. Rev. E **47**, R788 (1993); J. Fluid Mech. **278**, 123 (1994).

[10] A. Kudrolli, B. Pier, and J.P. Gollub, Physica D **123**, 99 (1998).

[11] H. Arbell and J. Fineberg, Phys. Rev. Lett. **85**, 756 (2000); **84**, 654 (2000).

[12] C. Wagner, H.W. Müller, and K. Knorr (unpublished).

[13] P. Debye, *Polar Molecules* (The Chemical Catalog Co., Dover, London, 1945).

[14] D. Roth, M. Lücke, M. Kamps, and R. Schmitz, Phys. Rev. E **50**, 2756 (1994).